



Research article

Effects of black cumin-based antimalarial drug loaded with nano-emulsion of bovine and human serum albumins by spectroscopic and molecular docking studies

Priyadarshini Mohapatra^b, Natarajan Chandrasekaran^{a,*}^a Centre for Nanobiotechnology, Vellore Institute of Technology, Vellore 632014, India^b Centre for Nanobiotechnology, Vellore Institute of Technology, Vellore, India

ARTICLE INFO

Keywords:

Human serum albumin
Bovine serum albumin
Thymoquinone
Mefloquine hydrochloride
Molecular docking

ABSTRACT

The growing understanding of nanoemulsion biomedical applications necessitates a basic understanding of protein–drug-loaded nanoemulsion interaction. In our present study, we investigated the binding interactions of Mefloquine (MEF)-loaded black cumin seed oil (Thymoquinone) nanoemulsion of different concentrations towards human and bovine serum albumin (HSA&BSA). Fluorescence emission, three-dimensional spectra, UV–visible spectroscopy, and FTIR-spectroscopy, techniques were used together with molecular docking studies to identify the binding effects. The ground state complex formation between Mefloquine-loaded black cumin seed oil nanoemulsion and protein fluorophores was confirmed by a decrease in fluorescence intensity and disputed hyper-chronicity found in the UV–visible spectra of albumins. According to three-dimensional fluorescence spectral analysis, the addition of MEF in thymoquinone impacted the microenvironment around aromatic amino acid (tryptophan and tyrosine) residues in HSA. The quenching mechanism is determined to be static contact by Stern–Volmer analysis, resulting in the formation of a stable bioconjugate. Significant modifications in the amide FTIR frequencies at around 1600 cm^{-1} correlate to variations in the secondary alpha-helical structures of biomolecules at the MEF-loaded nanoemulsion interface. Molecular dynamic studies have shown the binding affinity scores of the proteins BSA and HSA with the drug, MEF-loaded black cumin seed oil nanoemulsion. The determined thermodynamic parameters were found to agree with molecular docking data, indicating that van der Waals and hydrogen bonding forces were important in the interaction process. MEF prefers a highly polar binding site at the exterior area of domains in HSA than BSA, as shown in the molecular model, and the hydrogen bonds are highlighted. From our results, we have observed that drug delivery has a detrimental effect on protein frame confirmation by altering its physiological function.

1. Introduction

In order for the injected active component to be sufficiently dispersed in the aqueous environment and available at the site of action throughout the body, the process of drug delivery must be abided [1]. A variety of colloidal systems, including liposomes, solid lipid nanoparticle systems, emulsions, nanoemulsions and microemulsions, have been developed as drug delivery vehicles [2]. Oil/water

* Corresponding author.

E-mail addresses: nchandrasekaran@vit.ac.in, nchandra40@hotmail.com (N. Chandrasekaran).<https://doi.org/10.1016/j.heliyon.2022.e12677>

Received 14 November 2022; Received in revised form 15 December 2022; Accepted 21 December 2022

Available online 3 January 2023

2405-8440/© 2022 Published by Elsevier Ltd. This is an open access article under the CC BY-NC-ND license (<http://creativecommons.org/licenses/by-nc-nd/4.0/>).

nanoemulsion, for example, have a lot of promise for delivering poorly water-soluble drugs because of their many advantages, including ease of fabrication, increased drug loading, improved drug solubility and bioavailability, reduced patient variability, controlled drug release, and resistance to enzymatic degradation [3]. The nanoemulsion segmented hydrophobic and hydrophilic domains aid in the assimilation of polar and non-polar molecules [4].

Essential oils made from plants include bioactive components by nature, making them considered safer than synthetic goods for usage in the food and pharmaceutical industries [5]. Several studies have suggested that nanoemulsion could be used as a carrier for targeted drug delivery, as a preventive measure in bioweapons incidents, as an adjuvant for mucosal vaccines, as a non-toxic disinfectant cleaner, and for oral drug delivery [6]. As a result, the nanoemulsion in our work were made using the oils indicated above, which contain considerable bioactive chemicals, and their interactions with biomolecules were studied [35,41]. It could reveal details about the negative effects of using the nanoemulsion technologies described above as drug delivery vehicles within the body [7]. In summary, nanocarrier interactions with proteins cause structural conformational changes by exposing novel epitopes on the protein's surface [8]. As a result, research into the interaction of essential oil-based nanoemulsions with biological proteins has emerged as a major topic in biomedical research, with the goal of learning more about the structural changes that can occur [9–11]. In blood plasma, serum albumin is still the most abundant carrier protein. They aid in the transport and distribution of both exogenous and endogenous materials in the bloodstream [12].

Bovine serum albumin (BSA) is a protein found in blood plasma that aids in the disposition and transportation of several nutrients [13]. Human serum albumin (HSA) is still the most abundant soluble protein in the circulatory system [14]. The higher range of molecules, it has excellent acceptor capabilities. They are crucial in the development of new therapeutic agents, the prediction of drug pharmacokinetic behaviour, and the modulation of pharmacodynamics [15]. The sequences of BSA and HSA are 76% identical. The number of tryptophan residues is the main difference between them. HSA only has one tryptophan residue (W131), whereas BSA has two (W131 and W214) (W214) [16]. The major intrinsic fluorophores in serum albumins are tryptophan, tyrosine, and phenylalanine [17]. In comparison to phenylalanine, tryptophan and tyrosine residues contribute higher quantum yield in practical measurements [12]. As a result of such binding interactions, the intramolecular forces that govern the secondary structure of proteins may be altered, resulting in conformational changes in the protein [18]. Many drugs have had their ligand interactions with bio macromolecules studied such as anti-malaria drugs are a significant subset of these drugs [19]. Any change in the bio macromolecule's structure or function can be considered a drug's side effect [20]. Drug interactions with bio macromolecules like HSA & BSA can also affect their bioavailability and circulating lifetimes [21]. Strong interactions result in a decrease in the free fraction of drugs in plasma, while weak interactions result in a shorter lifetime and poor drug distribution [22]. MEF is an antimalarial drug that has been approved by the FDA and is currently used to treat malaria [23]. It is a quinine derivative that aids in the attack on Plasmodium during the intra erythrocytic stage of the parasite's life cycle. As a result, MEF has an advantage in treating *P. falciparum* malaria which is resistant to chloroquine.

Sekar et al. investigate how blood proteins and nanoemulsion interact, binding pattern concerning potential changes in the serum albumin nanoemulsion complex's structural conformation. They are more suited for in situ biomolecule collection and non-destructive measurement since they are highly sensitive, reasonably simple, and sensitive overall. A few studies have suggested that the variation in the protein folding and aggregation mechanism is caused by the protein binding on nanosurfaces [24]. According to research on biomolecules according to their physico-chemical properties, nanoparticles such as fullerene, CNTs, polymeric and fluorinated ones [25], have been shown to significantly alter the amyloid fibrillation pathway. According to a structural study, curcumin binds to BSA through polypeptide polar groups and has significant binding constants. It has been proven that trapping curcumin in nanoformulation prevents its hydrolysis [26]. The technology demonstrated delayed constant release and 99% encapsulation efficacy. In vivo investigations on pharmacokinetics, biodistribution, vasodilation, and toxicity inhibitory effects on the growth of tumor tissue will be used to determine the formulation's safety and effectiveness [27].

In previous research, we developed essential oil-based nanoemulsions and investigated their interaction with human serum albumins [28,29]. The study revealed that possible binding cum structural changes and biosafety studies as a result of the interaction process [30]. We used commonly spectroscopic methods to derive the binding pattern of serum albumin, MEF-loaded black cumin seed (Thymoquinone) oil-based nanoemulsion complex in conjunction with possible structural conformation disturbances. Optical techniques such as UV-Visible spectroscopy, fluorescence spectrophotometry, and Fourier transform infrared spectroscopy were the most commonly used among the various techniques to study molecular interactions [11,27,31]. However, no research has been done on the antimalarial drug (MEF)-loaded black cumin seed (Thymoquinone) nanoemulsion to bind to serum albumin proteins. We aim to present an extensive study of the interactions between MEF-loaded black cumin seed oil nanoemulsion (Thymoquinone) with HSA and BSA, which includes not only assessing the strength but also how the drug-loaded nanoemulsion binds to the protein, as well as structural alterations and the drug-protein binding site. We anticipate that the current investigation will provide important insights into the biological and therapeutic effects of MEF-Thymoquinone as well as the impact of biosafety on pharmacology. This study offers a persuasive viewpoint on how body's carrier protein is affected by nanophase medication delivery (serum albumin).

2. Materials & methods

Bovine serum albumin and human serum albumin were obtained from HI Media, India. Phosphate buffer of pH 7.2 bought from Sigma-Aldrich, USA. Nagila Sativa (Black cumin seed) oil bought from Sigma-Aldrich, Tween 80 (sorbitan monolaurate) was obtained from S.D.-Fine Chem. Limited, Mumbai. USA. Mefloquine hydrochloride was procured from Sigma-Aldrich, USA. Milli-Q water. All chemicals are of analytical grade. Excess Mefloquine was added to black cumin seed essential oil and vortexed for 15 min [32]. The sample was shaken for 72 h in an orbital shaker after the observation to dissolve the Mefloquine in black cumin seed essential oil [33]. The undissolved Mefloquine centrifugation at 3000g rpm (spin win, Tarson product Pvt. Ltd) was used to separate the water from the

oil [34]. The physical solubility was then investigated, and Mefloquine in the form of a pellet was found to be undissolved. Subsequently, 1 mg/mL of drug-loaded NE was selected as the ideal dosage for further description and implementation.

2.1. Nanoemulsion preparation

The drug loaded nanoemulsion was made with Black cumin seed oil (6% v/v), non-ionic surfactant, “Tween 80” and MilliQ [35]. The final concentration of Mefloquine hydrochloride in Black cumin seed oil was 1 mg/mL. MEF-loaded black cumin seed oil and surfactant properly mixed for 30 min at 250 rpm using a magnetic stirrer [3]. After formulation, it was sonicated using an ultrasonicator emulsifier (Sonics, Vibra cell line, USA) for 10 min at 20 kHz with a 40% amplitude [36]. The sample container was placed in an ice bath during the ultrasonication process to keep it cool. Before being used in characterization experiments, a clear MEF-loaded nanoemulsion was left at room temperature for one night to observe phase separation [37].

2.2. Characterization

2.2.1. Thermodynamic study

The thermodynamic stability of the MEF-loaded nanoemulsion was investigated in an order to ensure the physical stability. Such as, Centrifugation: The prepared drug-loaded nanoemulsion was centrifuged for 30 min at 7000 rpm to check for any phase separation [38]. The heating-cooling cycle was carried out for three times, with the temperatures being set at 45 and 4 °C for 48 h each time. At 20 and 25 °C, 48-h freeze-thaw cycles were carried out for triplicate [39].

2.2.2. Droplet size and polydispersity index

Dynamic light scattering (DLS) analysis is used to determine the droplet size distribution and polydispersity index (PI) of MEF-loaded nanoemulsion. (HITACHI, USA). Prior to analysis, the samples have been diluted with “double-distilled” water in a 1:30 ratio before analysis to reduce the effects of multiple scattering [2].

2.2.3. Turbidity studies

The turbidity of MEF-loaded nanoemulsion was measured at 600 nm using a UV–Visible spectrophotometer (HITACHI, U-2910)). Prior to the experiment, the samples were diluted in a 1:10 ratio with double distilled water to decrease turbidity [40].

2.3. Spectroscopic measurements

2.3.1. UV absorption

UV spectrophotometric absorbance measurements were carried out with a 0.1 nm resolution twin beam spectrophotometer. In the spectral range of 250–350 nm, the absorbance of BSA and HSA was determined. Samples were allowed to interact with diluted MEF loaded nanoemulsion concentrations, such as 2–10 μl [41].

2.3.2. Intrinsic fluorescence spectroscopy

Fluorescence spectra were recorded using a spectrofluorometric (Jasco FP-6500) with a quartz cuvette (10 mm path length) filled with a protein solution and placed in a thermostatically controlled cell holder [18]. For the fluorescence measurements of MEF-loaded black cumin seed nanoemulsion, with a standard solution of BSA and HSA was allowed to interact with varying concentrations, such as 2–10 l in the orbital shaker for 5 min [42]. A stern-volmer plot was created from the fluorescence spectra by plotting the volume of the drug-loaded nanoemulsion along with the ratio of BSA and HSA’s fluorescence intensities before and after their interaction with the drug-loaded nanoemulsion system [43].

For spectral measurements, the following settings were used: excitation and emission bandwidths of 5 nm each; $\lambda_{ex} = 333$ nm; $\lambda_{em} = 300$ –500 nm; detector voltage = 240 V; scan speed = 500 nm min⁻¹; and data pitch = 1 nm. The ratio of the fluorescence intensity of BSA and HSA before and after contact with the oil nanoemulsion system, along with the nanoemulsion volume on the x-axis, was used to make the Stern-Volmer plot from the fluorescence spectra [16].

The fluorescence spectra (at $\lambda_{max} = 333$ nm) were analysed using the stern-volmer equation (1) [13]:0

$$\frac{F_0}{F} = 1 + k_{sv}[Q] \quad (1)$$

where F_0 is the intensity of free HSA/BSA fluorescence and F is the intensity of HSA/BSA fluorescence after interaction with MEF-black cumin seed nanoemulsion. Stern–volmer quenching constant and drug concentration are denoted by k_{sv} and $[Q]$, respectively. F_0/F against MEF-loaded black cumin seed nanoemulsion concentration graphs were created. The k_{sv} is calculated using the linear regression of this plot. The graphs of $\log(F_0 - F)/F$ is $\log [MEF-BMC]$ were also plotted and used to calculate the binding constant (K_b) and the number of binding sites (n) using the modified stern–volmer equation-(2) [29,30].

$$\frac{\log}{BMC} = \log k_b + n \log [Q] \quad (2)$$

Table 1
Physicochemical characterization of formulated drug-loaded nanoemulsion.

Parameter	Black cumin seed NE	MEF-Black cumin seed NE
z-Average/Zeta potential	72.9nm/-2.5 mV	86.1nm/-2.8 mV
Polydispersity Index	0.154 ± 0.0014	0.189 ± 0.0024
Thermodynamic stability	Stable	Stable
pH	6.98 ± 0.21	6.23 ± 0.58

2.3.3. Three dimensional (3D) fluorescence spectra

Using the experimental parameters listed in the instruction manual, the three-dimensional fluorescence spectra of HSA and BSA were measured [9,28]. The start and end wavelengths of excitation and emission were adjusted at 300 and 500 nm, respectively [18]. The sampling intervals for excitation and emission were adjusted to 30 and 10 nm, respectively. The scan speed stays at 60,000 nm min⁻¹ and the voltage remained at 360 V, at 5 nm the excitation and emission slits were fixed [14]. Drug-loaded nanoemulsion was present or absent from the contour plot of biomolecules. Between the emission and excitation wavelengths, the Stokes shift (nm) was calculated.

2.3.4. Fourier transform infrared (FTIR) spectroscopy

It analysis of control (BSA&HSA) and MEF loaded-nanoemulsions interacted with protein (BSA&HSA) samples are performed at a resolution of 1. The device includes a KBr and Mylar beam splitter, and the powder mixed with KBr was compressed into to pellets under low pressure (1.5psi). At 25 ± 3 °C, the spectrum was measured from 4500 to 400 cm⁻¹. The control sample (BSA&HSA) and MEF loaded nanoemulsion interacted with BSA& HSA were examined to evaluate any potential changes to the amide areas that correspond to the structural shape of the helical filament.

2.4. Data curation

2.4.1. Protein receptor data set curation

The protein 3D structure was downloaded for Bovine Serum Albumin (BSA) protein along with the 3D coordinates from Protein Data Bank (PDB) database (<https://www.rcsb.org/>) with a PDB ID: 4F5S [44]. The obtained protein structure is a monomeric molecule with a single unique chain. Whereas, the Human Serum Albumin (HSA) protein does not have any available 3D structures in the PDB database. We have retrieved the protein sequence for HSA from the UniProt protein sequence database and modeled the protein using the Swiss-Model online server [45]. The model has been generated using the templet with 90% similarity scores. The modeled protein is further used for protein refinement and docking analysis.

2.4.2. Protein refinement

Prior to molecular docking, the Pymol tool was used to further improve the protein structures by eliminating the crystallographic water molecules and undesirable heteroatoms [46]. The non-standard residues including the water molecules, ligand, phosphate, and sulphate groups should be removed for the successful completion of the docking procedure using Autodock tools.

2.4.3. Ligand dataset curation

The drug bank database (<https://www.drugbank.com>) and PubChem compound database (<https://pubchem.ncbi.nlm.nih.gov/>) of the National Center for Biotechnology Information (NCBI) was used to download the ligand structures [47]. The ligand molecules (Mefloquine and Thymoquinone) structures were retrieved from the Drug bank database.

2.4.4. Protein-ligand docking analysis

The protein structures were further prepared as per the Autodock tool docking protocol. Polar hydrogen atoms were added and non-polar hydrogen atoms were merged followed by adding Kolman charges to the protein molecule. The ligand molecule was also prepared as per the protocol and saved the ligand molecule as "ligand.pdbqt" file format. Autodock-Grid algorithm is used for preparing the grid around the protein molecule. A genetic algorithm is used for the protein-ligand docking process as a part of the standard docking protocol of Autodock-Dock [30]. The best-docked complex for each set of dockings is selected based on the binding affinity scores and the binding orientation has been visualized using discovery studio.

2.4.5. Protein-ligand complex visualization and analysis

The complex is visualized using the discovery studio [11]. The binding positions for each set of docking were captured and the binding amino acids were identified. The binding forces helpful for stabilizing the protein-ligand were analysed using the Discovery studio tool. Discovery studio facilitates to visualization of the Hydrogen bonds along with the other stabilizing bonds such as the hydrophobic interactions and van Der Waals interactions.

3. Result and discussion

The results of physicochemical characterization of the formulated drug-loaded nanoemulsion are provided in Table 1. The visual

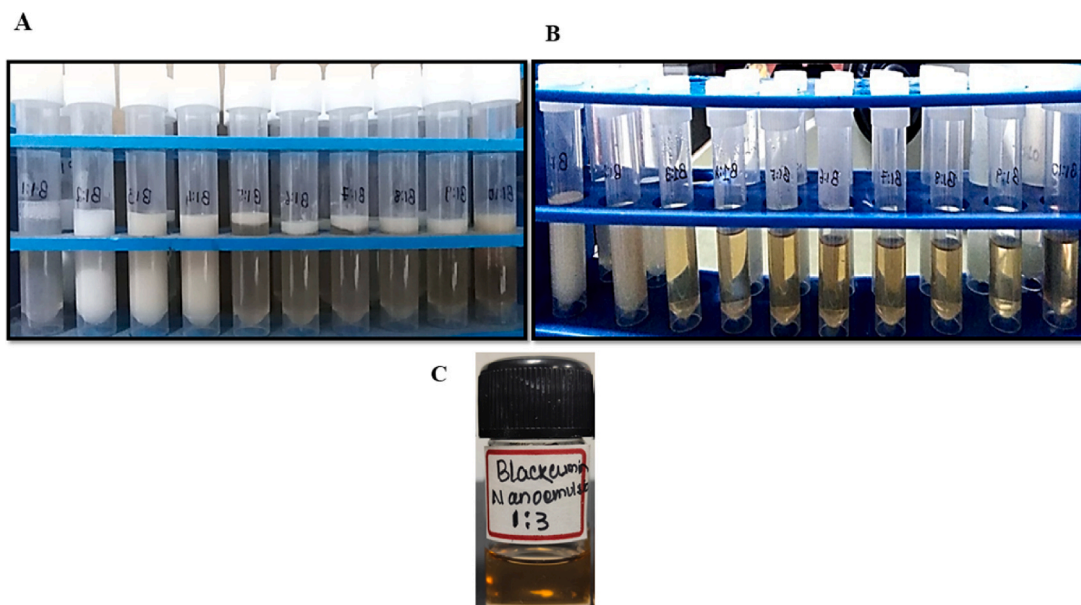


Fig. 1. Visual appearance of formulated MEF loaded Black cumin seed oil Nano emulsion (A: Coarse Emulsion of Black cumin seed oil, B: Nano formulation of Black cumin seed oil, C: Mefloquine loaded Black cumin seed oil Nanoemulsion(1:3 ratio)).

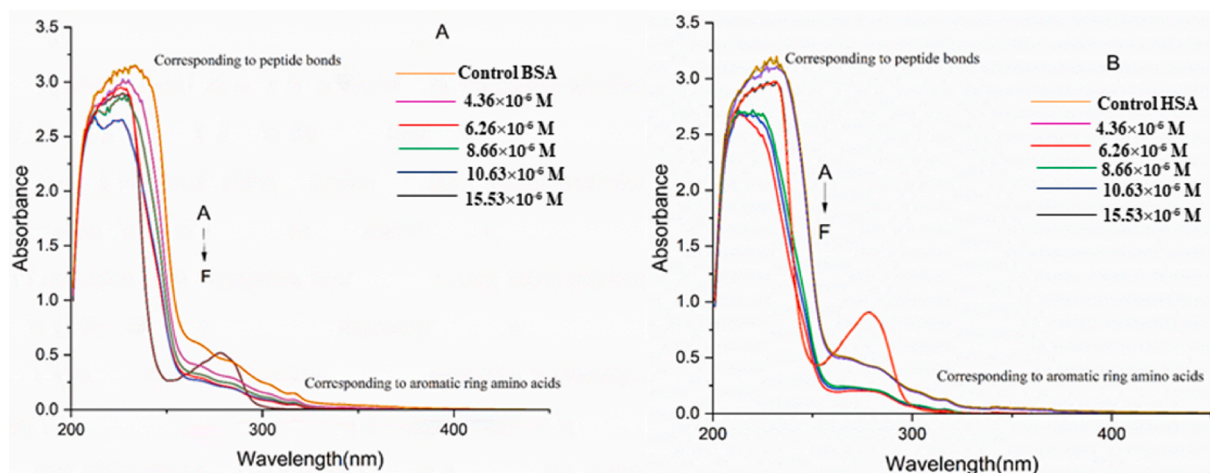


Fig. 2. UV-Visible spectroscopy in the interaction of BSA and HSA (0.01%) produced in a phosphate buffer with a pH of 7.2 and increasing volumes of MEF-loaded black cumin nanoemulsion systems.

appearance of coarse emulsion Fig. 1(A), nanoemulsion Fig. 1(B) and MEF-loaded nanoemulsion of black cumin seed oil had in Fig. 1(C). The UV Visible Spectrophotometer at 600 nm revealed that the Black cumin seed nanoemulsion has a percent transmittance of more than 90%, indicating that the emulsion is optically transparent and size dependant. Because of the smaller droplet size, the emulsion is less turbid Fig. 1(B & C). The coarse emulsion initially had larger droplet sizes in the 100–300 nm range and was milky white in colour Fig. 1(A) [48]. Initially, the coarse emulsion Fig. 1(A) was milky white with bigger droplet sizes in the 100–300 nm range.

Ultra-sonicated MEF-loaded black cumin seed oil nanoemulsions were very clear and less viscous Fig. 1(C), with a 50–100 nm size range. For the emulsification and dispersion of substances, the food and pharmaceutical industries frequently use “Tween 80” (HLB = 15), a non-ionic hydrophilic surfactant. As illustrated in Table 1, the mean droplet diameter of the formed nanoemulsion and drug-loaded nanoemulsion was to be 72.9 nm and 86.1 nm, respectively, with polydispersity indexes (PDI) of 0.154 and 0.189 as determined by dynamic light scattering (DLS). Both nanoemulsions had PDIs smaller than 0.5, indicating that the emulsions were homogeneous [36,49]. The zeta potential value of black cumin seed nanoemulsion and MEF loaded Black cumin seed nanoformulation were depends upon the surfactant used in the nano-formulation [50,51]. As mentioned in the study in zeta potential and particle size measurements, single and binary mixtures of non-ionic and ionic surfactants were used. However, there were noticeable differences between the surfactants, such as how nonionic surfactants reduced the absolute magnitude of zeta potential of powders in a pH range

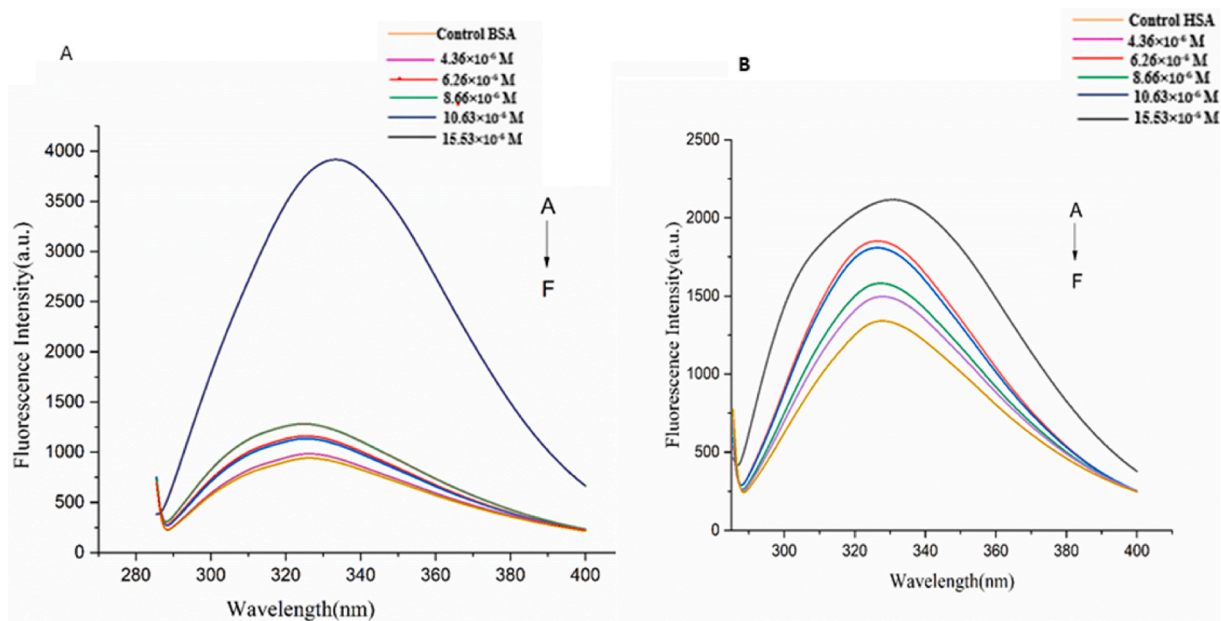


Fig. 3. BSA and HSA fluorescence emission spectra in the presence of MEF loaded nanoemulsion made of (A) BSA-MEF loaded black cumin loaded nanoemulsion (B) HSA- MEF loaded black cumin seed oil nanoemulsion. The peak shift and decreasing intensity support the BSA and HSA's affinity for the drug loaded nanoemulsion surface.

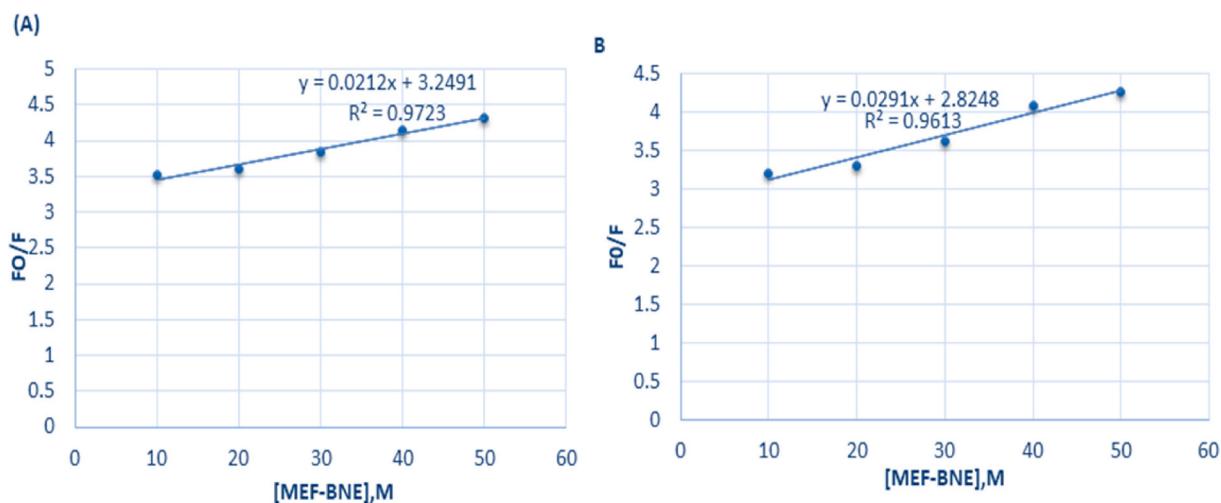


Fig. 4. (A) BSA-MEF loaded Black cumin loaded nanoemulsion (B) HSA- MEF loaded Black cumin seed oil nanoemulsion conjugate system stern-volmer plots. I_0/I versus nanoemulsion volume shown in a linear fashion. The graph's Ksv and Kq values are included in the text.

of 2.0–11 [25]. Because of the presence of non-ionic surfactants, the absolute values of zeta potential are expected to be relatively low despite being in the stable range. It has been reported that the presence of non-ionic surfactants reduces the magnitude of zeta potential over a wide pH range [52]. Both emulsion's thermodynamic stability was stable as evidenced from the heating cooling cycle process at varied temperatures, with no notable variations in size [53]. As high pH generates oil-in water emulsion, it was verifying from the provided pH value in table-1 [3].

3.1. UV -absorption

UV Visible spectroscopy is the most efficient tool for investigating protein absorbance [14]. In the absorption spectrum of BSA and HSA, a broad peak at 280 nm and 295 nm corresponds to transitions in the aromatic rings of Tryptophan(Trp), Tyrosine (Tyr) and Phenylalanine (Phe) residues. In Fig. 2(A&B), as the BSA & HSA-MEF loaded in Black cumin seed nanoemulsion containing solution

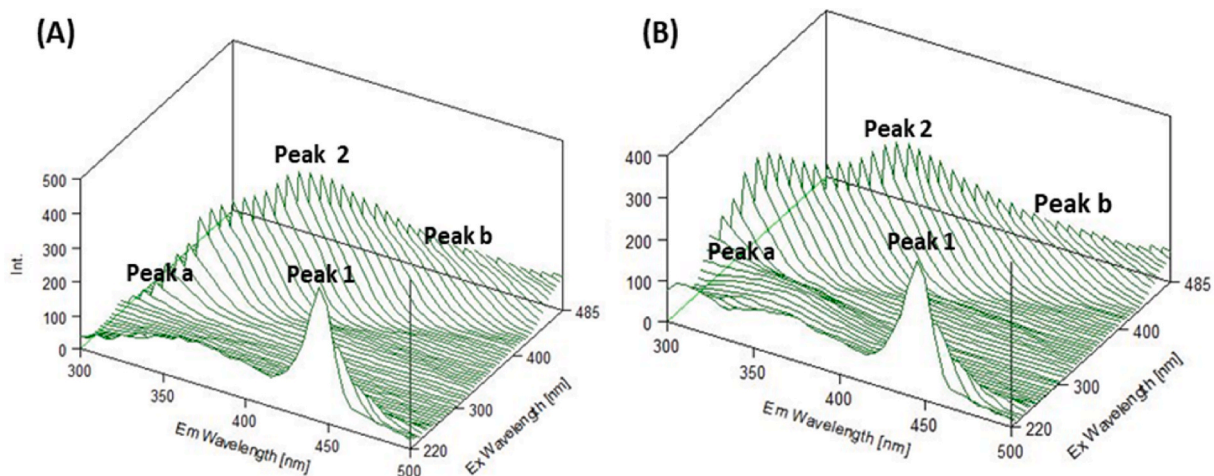


Fig. 5. Three-dimensional spectra of BSA and HSA before after it interacts with, respectively(A) BSA (Control) (B) BSA- MEF loaded Black cumin seed oil nanoemulsion.

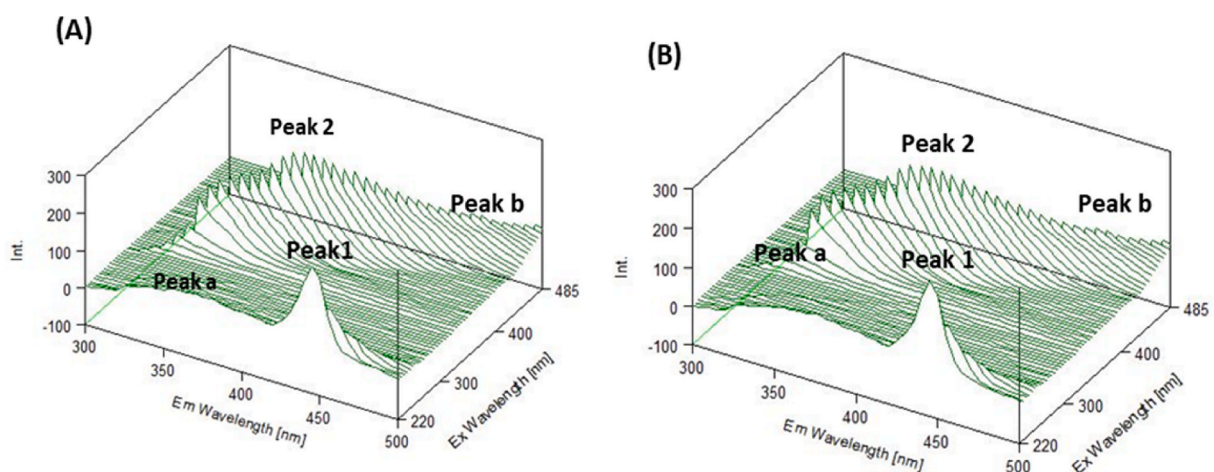


Fig. 6. Three-dimensional spectra of BSA and HSA before after it interacts with, respectively(A) HSA (Control) (B) HSA- MEF loaded Black cumin seed oil nanoemulsion.

increases, so does the absorption strength of this peak, confirming the changes in protein framework structure in the presence of the MEF loaded Black cumin loaded nanoemulsion [16]. The graph depicts the sample composition of drug-loaded nanoemulsion with BSA and HSA, Milli Q to calculate the final volume, which is shown in Fig. 2. Both protein-ligand interaction studies at constant concentration produced a distinct peak. This could be due to the duration of the interaction or the binding effect. Protein has a maximum absorbance of roughly 280 nm in general [54]. This originates from the π - π transition of aromatic amino acid residues such as tryptophan and tyrosine. The aromatic microenvironment of amino acid residues affects the molecular conformation of proteins [13]. Furthermore, changing the maximum wavelength to longer wavelengths (redshift) shows an increase in the hydrophobicity of the environment around Trp and Tyr [55]. In the ground state, the complex's affinity would have exposed the aromatic bonds and raised the molecule's UV absorbance. As a result, biomolecules' UV-visible spectra shift in response to changes in their microenvironment [15].

3.2. Fluorescence spectroscopy

The mechanism of black cumin seed oil nanoemulsion –BSA & HSA interaction was investigated in this paper by measuring changes in the biomolecule's intrinsic fluorescence spectra. Fig. 3(A&B) shows MEF-loaded black cumin seed oil nanoemulsion increases on BSA as well as HSA fluorescence intensity(FI), indicating that the intensity of fluorescence of BSA and HSA reduces as MEF-loaded black cumin seed oil nanoemulsion concentration increases. When HSA was excited at 290 nm, its fluorescence intensity (FI) peaked at 334 nm. There was a red shift from 334 to 337 nm in HSA and 320–324 nm BSA after adding MEF loaded Black cumin nanoemulsion oil nanoemulsion. When MEF was added to the HSA solution, the FI at 343 nm gradually decreased and at the highest

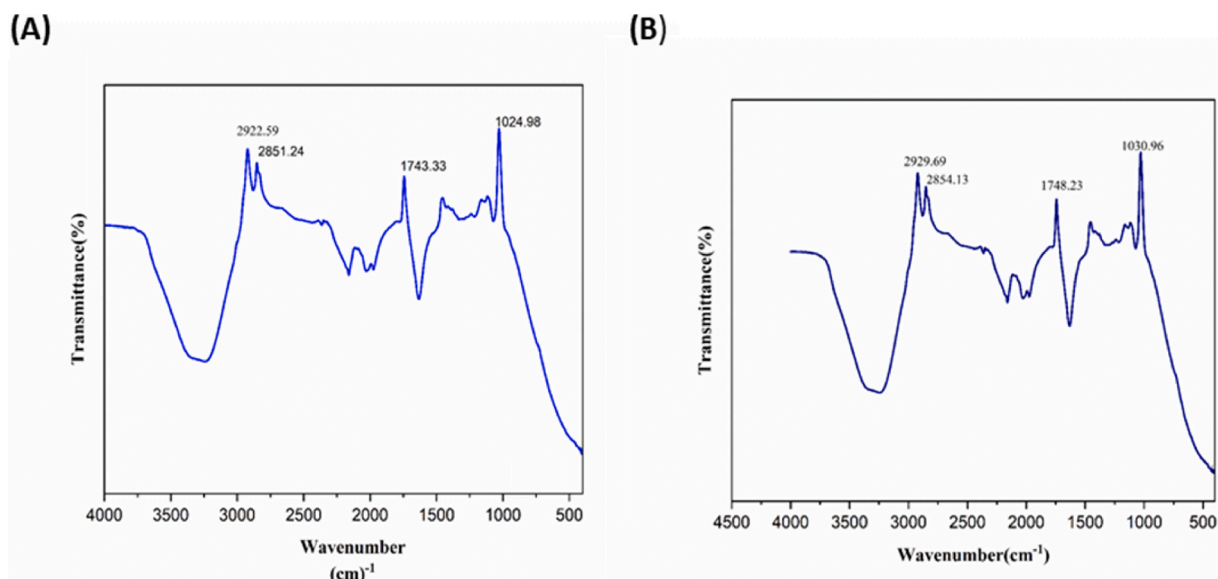


Fig. 7. FTIR of (A) BSA (Control) (B) BSA- MEF loaded Black cumin seed oil nanoemulsion. The secondary structure of BSA changes in response to changes in the amide band.

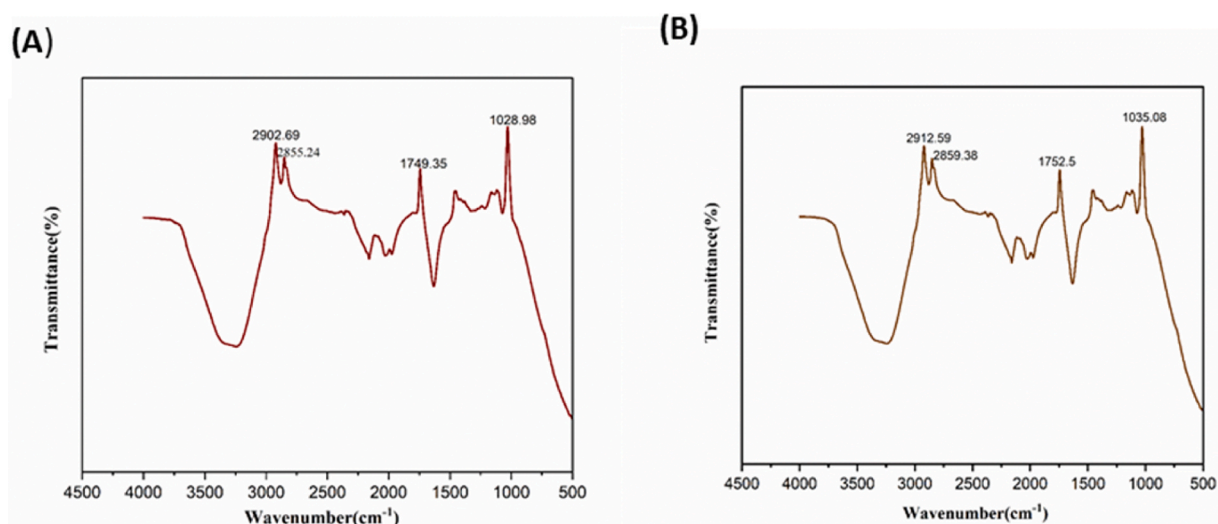


Fig. 8. FTIR of (A) HSA (Control) (B) HSA- MEF loaded Black cumin seed oil nanoemulsion. The secondary structure of BSA changes in response to changes in the amide band.

Table 2

Peaks of BSA and HSA in the absence and presence of MEF-loaded black cumin seed Nanoemulsion.

BSA(control) (cm ⁻¹)	HSA(control) (cm ⁻¹)	BSA-MEFloaded Nanoemulsion(cm ⁻¹)	HSA-MEFloaded Nanoemulsion(cm ⁻¹)	Band Assignment
2922.59	2902.69	2929.59	2912.59	Amide-A NH stretching
2851.24	2855.24	2854.13	2858.38	CH stretching
1743.33	1749.35	1746.23	1752.33	Amide-I C1/4 O stretching
1024.98	1028.98	1029.98	1035.08	Secondary Amine CN Stretching

MEF concentration (27 M), a 49% percent reduction in the FI was observed [9]. 27 M concentration of Mefloquine in the sample with BSA and HSA, In the figure it was mentioned the total concentration of drug-loaded formulation with protein compounds. In addition, at 27 M MEF concentration, there was a slight (2 nm) blue shift in HSA emission maxima. The binding of the protein's tryptophan

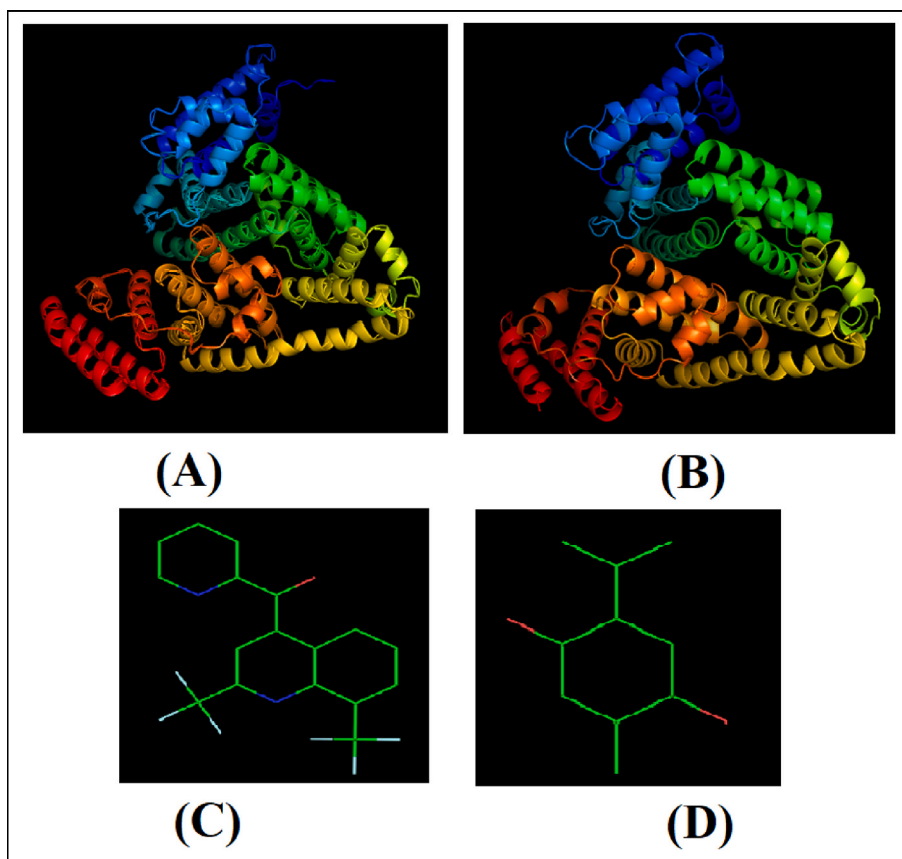


Fig. 9. The 3D structures of the protein and ligand molecules visualized using Pymol visualization tool. A) 3D structure of Bovine Serum Albumin (BSA) protein. B) 3D structure of Human Serum Albumin (HSA) protein. C) 3D structure of Mefloquine drug molecule. D) 3D structure of Thy-moquinone drug molecule.

residues to the nanoemulsion surface so, it also shows that the tryptophan residues found in the native protein's hydrophobic core region are exposed to solvent. The increased interaction of drug-loaded nanoemulsion systems with chromophore residues, combined with changes in the molecular environment surrounding them, has resulted in a quenching effect with a significant blue shift. Where $[Q]$ is the nanoemulsion concentration, K_{sv} is the Stern-Volmer quenching constant, and I_0 and I are the fluorescence intensities of HSA and BSA in the absence and presence of different nanoemulsion systems, respectively [28].

The plot of I_0/I versus nanoemulsion-loaded drug concentration must be linear, according to the Stern-Volmer model of binding [30]. As demonstrated in Fig. 4(A and B), our BSA and HSA interact with MEF-loaded black cumin seed oil nanoemulsion data to fit the Stern-Volmer plot well and achieve good linearity. The K_{sv} (MEF-loaded black cumin seed oil-based nanoemulsion-HSA&BSA systems) were found to have values of 0.0212 and 0.0358 ($l \text{ mol}^{-1}$) based on the slope of the linear equation of the stern-volmer plot., respectively based on the Stern-Volmer plot's linear equation's slope. K_{sv} is equal to the product of K_q and τ_0 in the equation, where K_q is the collisional quenching binding constant of nanoemulsion-protein conjugates and Without any quencher, the average biomolecule lifetime is K_{sv} (1×10^{-8} s). As a result, the K_q values of MEF loaded Black cumin seed oil nanoemulsion – BSA & HSA conjugates were calculated to be 1.36×10^{-8} and 2.01×10^{-8} ($l \text{ mol}^{-1} \text{ s}^{-1}$), respectively. Where K is the binding constant, n is the number of binding sites, I_0 and I are the fluorescence intensities in the presence and absence of a quencher, Q is the concentration of the MEF-loaded Black cumin seed oil nanoemulsion in molar units [29]. The higher the correlation coefficient, the closer it is to one, indicating the presence of independent binding sites. UV-Visible spectral data will be used to determine the precise quenching mechanism between the nano-bio conjugates [15]. In general, quenching mechanisms can be divided into two types: dynamic and static [16]. In contrast to static quenching, dynamic quenching achieved through collision and energy transfer does not produce any change in the UV spectrum of biomolecules upon engagement with the quencher [9]. The UV-Visible absorbance and fluorescence emission of both nanoemulsion systems varied, indicating that the mechanism is static in nature. Regardless of the mechanism, fluorescence emission spectra were effective in obtaining information about changes in the protein's aromatic microenvironment [12].

3.3. Three dimensional (3D) fluorescence spectra

Biomolecular three-dimensional spectroscopic examinations give thorough details on fluorescence and structural alterations. The

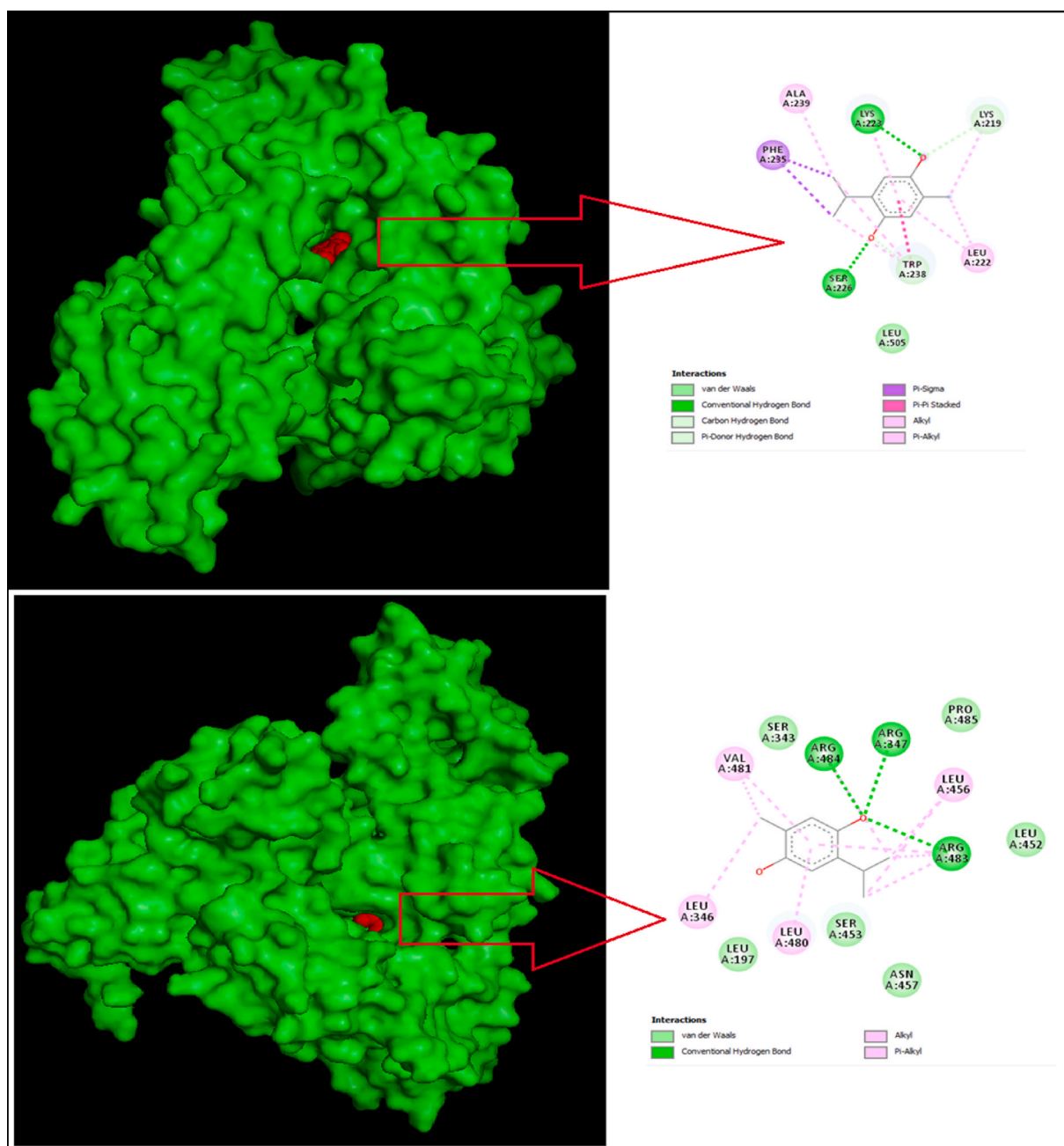


Fig. 10. Docking of BSA and HSA protein receptors with the Thymoquinone drug molecule were visualized using Discovery studio: A) The interacting amino acid residues and the binding affinity scores of the BSA vs. Thymoquinone complex. B) The interacting amino acid residues and the binding affinity scores of the HSA vs. Thymoquinone complex.

Table 3

Molecular docking results. Energies of hydrogen bonds in the interaction process between Thymoquinone and Mefloquine responsive amino acids.

Amino Acid	Energy (kcal mol ⁻¹)	Bond Length (Å)	Hydrogen Bond
ARG347	-0.55	1.3	2
SER226	-0.53	2.4	2
TYR149	-0.23	5.9	2
ARG210	-0.27	4.3	2

Table 4
Molecular docking results. BSA and HSA interaction with Thymoquinone-Mefloquine.

Pose	BE(BSA) (kcal mol ⁻¹)	BE(HSA) (kcal mol ⁻¹)
1	6.06	-7.03
2	5.09	-6.98
3	5.48	-6.01
4	5.26	-5.75
5	5.24	-5.34
6	5.03	-5.11

contour view plots were used to express the biomolecules' 3D scan spectra in absence and presence of MEF-loaded nano-emulsion in this work. A contour map depicts the emission maxima of biomolecules as well as their associated excitation wavelength. The surface of the 3D map depicts a plot that illustrates not only biomolecules conformations change when they contact with nanoemulsions, but also the residues of aromatic amino acids [29]. The contour view spectra in Fig. 5 (A (control), 5 (B) is BSA-MEF loaded Black cumin seed oil nanoemulsion), and 6(A (control), 6(B) is HSA-MEF loaded Black cumin loaded oil nanoemulsion) describes the shifts in biomolecule emission spectra, as well as the wavelength shift. In Fig. 5(A&B), Fig. 6(A&B) describes about BSA (5A) and BSA-MEF loaded black cumin seed oil with Peak a, peak b, peak 1, and peak 2 are all present in each spectrum. The first Rayleigh scattering corresponds to peaks a and b where the maximum excitation (ex) equals the maximum emission (em) [15]. The aggregation of BSA and HSA onto the drug-loaded nano-emulsion surface was confirmed by a peak intensity increase during interaction with the nanoemulsion. As aggregation improves, the system's size grows, resulting in a better scattering mechanism. The emission maxima at 380 and 450 nm were seen in the contour plots of BSA and HSA (control) in Figs. 5A and 6A, with the excitation wavelength position of 420 nm. These peaks were determined to have values of 90 and 80 nm, respectively. The value did not change considerably while interacting with MEF-loaded nanoemulsion (the emission maxima did not shift significantly), but the intensity reduced, as shown in Fig. 5(A&B) and Fig. 6(A&B). Although the intensity of the spectra was found to diminish, neither (bovine nor human serum albumin) showed any significant changes in their values after interaction with MEF-loaded Black cumin seed oil nano-emulsion. These findings imply that the influence of MEF-loaded Black cumin oil nanoemulsion on serum albumins may affect their aromatic environment, as indicated by the fluorescence quenching data [30]. Furthermore, peak 2 of both albumins did not significantly change when they interacted with MEF loaded the Black cumin seed oil nanoemulsion surface, demonstrating that the contact phenomena are unsuccessful in altering the conformations of the peptide strands according to the 3D spectrum result. As a result, the three-dimensional spectra show that the action of MEF loaded Black cumin seed oil nanoemulsion is limited to the rather peptide conformation, tryptophan, and tyrosine residues have an aromatic microenvironment.

3.4. FTIR spectroscopy

Biomolecules' structural and conformational dynamics can be studied using FT-IR spectroscopy. In general, proteins have an amide I C1/4 O band between 1600 and 1700 cm⁻¹ that results at 1548 cm⁻¹, and an amide II band results from C=O stretching. This is due to the CN stretching and NH bending modes, and also to the amide III band size at 1300 cm⁻¹ [13]. The amide I band remains more prone to modifications in protein secondary structure than the amide II band. [40]. They exhibit a substantial connection between the structural conformation of the alpha-helical structure [16]. Despite the use of nanoemulsion systems, BSA and HSA displayed their amide A NH peaks at 2922.69 and 2902.69 cm⁻¹ in the current investigation, as shown in Figs. 7A & 8A.

However, when the peak was exposed to MEF-loaded black cumin seed oil nanoemulsion, BSA shifted 2922.59 to 2929.59 cm⁻¹ and HSA shifted 2902.69 to 2912.59 cm⁻¹, as seen in Figs. 7B & 8B. Additional peaks were observed in BSA and HSA at around 2855.24 and 2858.38 cm⁻¹ of CH stretching, 1746.23 and 1752.33 cm⁻¹ of amide I C1/4O band stretching, 1029.98 and 1035.08 cm⁻¹ of secondary amine CN stretching in contact with MEF-loaded black cumin oil nanoemulsion. The changes in the amide I band of BSA and HSA detected when they interacted with MEF-loaded black cumin seed oil nanoemulsion show that changes in biomolecule secondary structures are possible [15]. Table 2 contains all of BSA & HSA's FTIR peaks in the absence and presence of MEF-loaded black cumin seed oil nanoemulsion.

3.5. Analysis of computational studies

The protein 3D structures obtained from PDB database were visualized using Pymol tool. The drug molecules were obtained in ".mol2" file format and converted them to ".pdb" file format which is an acceptable file formats for the molecular docking procedure Fig. 9 (A,B,C,D).

The protein receptors BSA and HSA have shown binding affinity scores of -6.57 and -6.38 with the ligand molecule Thymoquinone. The analysis of binding forces for the complex has shown that the Thymoquinone has formed three hydrogen bonds with the amino acids ARG347 483 and ARG484 with a ligand efficiency value of -0.55, inhibition constant value of 15.35 μM whereas the HSA protein has shown two hydrogen bonds LYS223 and SER226 with a ligand efficiency value of -0.53, inhibition constant value of 21.05 μM. The 2D representation of protein-ligand binding of BSA with Thymoquinone is provided in Fig. 10A and HSA with Mefloquine in Fig. 10B (Table 3).

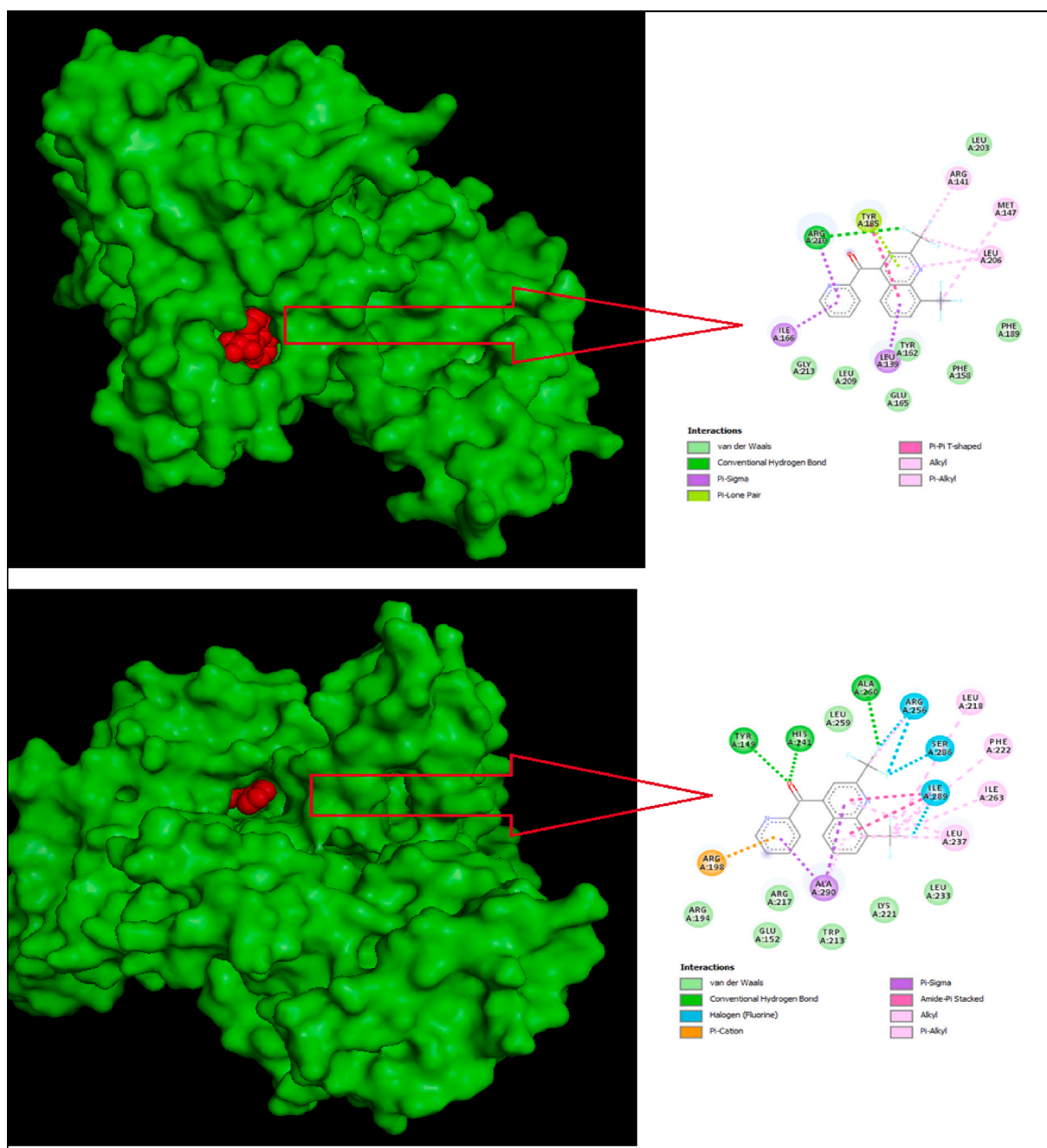


Fig. 11. Docking of BSA and HSA protein receptors with the Mefloquine drug molecule were visualized using Discovery studio: A) The interacting amino acid residues and the binding affinity scores of the BSA vs. Mefloquine complex. B) The interacting amino acid residues and the binding affinity scores of the HSA vs. Mefloquine complex.

In other docking studies, we have observed that BSA protein has shown a binding energy score of -6.06 with Thymoquinone ligand whereas the HSA protein has shown a binding energy score of -7.03 as (Table 4).

The analysis of binding forces for the protein-ligand complex has shown that Mefloquine has formed three hydrogen bonds with the amino acids TYR149, HIS241, and ALA260 with a ligand efficiency value of -0.23 , inhibition constant value of $36.15 \mu\text{M}$ whereas the HSA protein has shown two hydrogen bonds with ARG210 with a ligand efficiency value of -0.27 , inhibition constant value of $7.08 \mu\text{M}$. The 2D representation of protein-ligand binding of BSA with Mefloquine is provided in Fig. 11A and HSA with Mefloquine in Fig. 11B.

The molecular docking results have demonstrated that the protein HSA has shown better binding affinity scores than the BSA

protein when performed with the drug Mefloquine. From the results, we can assume that the Mefloquine drug along with the Thymoquinone drug can be more efficient when targeting the HSA. Our comparative studies have shown a significant variance in the binding affinity scores when docked with the two drugs used for the nanoemulsion.

4. Conclusion

In conclusion, we studied the mechanism of interaction between MEF-loaded black cumin seed nanoemulsion with HSA and BSA using a mix of spectroscopic and molecular modelling methods. The findings suggest that drug-loaded transport could unfold protein structure and increase chromophore group exposure in the interior hydrophobic area, resulting in a change in the microenvironment of amino acid residues. Incorporation of hydrophobic drugs in a topical formulation along with favorable patient compliance is not feasible, but nanoformulation form of the same drug does that efficiently. Rationalized formulation development of nanoformulation for various drugs could solve various problems related to drug solubility, stability, and drug release associated with other topical formulations [11]. The addition of reduces the α -helix content from 68.62% to 62.76%. They were eventually able to create a stable bioconjugate using hydrogen bonding. Furthermore, the binding site was discovered to be positioned at the domains. This study demonstrates that drug delivery has a detrimental effect on protein frame conformation, compromising its physiological properties. Given the influence on proteins, the biocompatibility of this drug-loaded delivery should be given greater consideration. This study not only shows that HSA and BSA interacts with MEF-loaded black cumin nanoemulsion, but it also gives a method for evaluating protein structure. Nevertheless, when it comes to analysing the harmful effect of drugs on proteins, the degeneration of physiological activities of proteins is a factor. Protein- The usage of drug-encapsulated nanoemulsion could enhance medication delivery, clinical implications for biosensing, therapeutic targeting, and other topics in the future.

Conflict of interest

The authors involved reveal no sources of conflict of interest.

Credit author Statement

1 - Conceived and designed the experiments- PriyadarshiniMohapatra, N.Chandrasekaran 2 - Performed the experiments- PriyadarshiniMohapatra, N.Chandrasekaran 3 - Analyzed and interpreted the data- PriyadarshiniMohapatra, N.Chandrasekaran 4 - Contributed reagents, materials, analysis tools or data-PriyadarshiniMohapatra, N.Chandrasekaran 5 - Wrote the paper- PriyadarshiniMohapatra, N.Chandrasekaran

References

- [1] C.A. Kruger, H. Abrahamse, Utilisation of targeted nanoparticle photosensitiser drug delivery systems for the enhancement of photodynamic therapy, *Molecules* 23 (2018), <https://doi.org/10.3390/molecules23102628>.
- [2] S. Sugumar, S.K. Clarke, M.J. Nirmala, B.K. Tyagi, A. Mukherjee, N. Chandrasekaran, Nanoemulsion of eucalyptus Oil and its Larvicidal Activity against *Culex quinquefasciatus*, 2014, pp. 393–402, <https://doi.org/10.1017/S0007485313000710>.
- [3] S. Sugumar, S. Singh, Nanoemulsion of Orange Oil with Non Ionic Surfactant Produced Emulsion Using Ultrasonication Technique : Evaluating against Food Spoilage Yeast, 2015, <https://doi.org/10.1007/s13204-015-0412-z>.
- [4] V. Ghosh, S. Saranya, A. Mukherjee, N. Chandrasekaran, Cinnamon Oil Nanoemulsion Formulation by Ultrasonic Emulsification : Investigation of its Bactericidal Activity, 2013, <https://doi.org/10.1166/jnn.2013.6701>.
- [5] K. Anwer, S. Jamil, E.O. Ibnouf, F. Shakeel, Enhanced Antibacterial Effects of Clove Essential Oil by Nanoemulsion, vol. 354, 2014, pp. 347–354.
- [6] S. Çalıř, K. Öztürk Atar, F.B. Arslan, H. Erođlu, Y. Çapan, Nanopharmaceuticals as Drug-Delivery Systems, *Nanocarriers Drug Deliv*, 2019, pp. 133–154, <https://doi.org/10.1016/b978-0-12-814033-8.00004-7>.
- [7] M. Jaiswal, R. Dudhe, P.K. Sharma, Nanoemulsion: an advanced mode of drug delivery system, 3 *Biotech* 5 (2015) 123–127, <https://doi.org/10.1007/s13205-014-0214-0>.
- [8] Y. Liu, H. Miyoshi, M. Nakamura, Nanomedicine for drug delivery and imaging: a promising avenue for cancer therapy and diagnosis using targeted functional nanoparticles, *Int. J. Cancer* 120 (2007) 2527–2537, <https://doi.org/10.1002/ijc.22709>.
- [9] K.A. Musa, N.F.W. Ridzwan, S.B. Mohamad, S. Tayyab, Combination mode of antimalarial drug mefloquine and human serum albumin: insights from spectroscopic and docking approaches, *Biopolymers* 111 (2020) 1–11, <https://doi.org/10.1002/bip.23337>.
- [10] O. Tarasova, V. Poroikov, A. Veselovsky, Molecular docking studies of HIV-1 resistance to Reverse Transcriptase Inhibitors: mini-review, *Molecules* 23 (2018) 11–13, <https://doi.org/10.3390/molecules23051233>.
- [11] H. Monirinasab, M. Zakariazadeh, H. Kohestani, M. Kouhestani, F. Fathi, Study of β -lactam-based drug interaction with albumin protein using optical, sensing, and docking methods, *J. Biol. Phys.* 48 (2022) 177–194, <https://doi.org/10.1007/s10867-021-09599-0>.
- [12] T. Cedervall, I. Lynch, M. Foy, T. Berggård, S.C. Donnelly, G. Cagny, et al., Detailed identification of plasma proteins adsorbed on copolymer nanoparticles, *Angew. Chem., Int. Ed.* 46 (2007) 5754–5756, <https://doi.org/10.1002/anie.200700465>.
- [13] Y.Z. Zhang, N.X. Zhang, A.Q. Ren, J. Zhang, J. Dai, Y. Liu, Spectroscopic studies on the interaction of 2,4-dichlorophenol with bovine serum albumin, *J. Solut. Chem.* 39 (2010) 495–510, <https://doi.org/10.1007/s10953-010-9518-9>.
- [14] K. Langer, M.G. Anhorn, I. Steinhauser, S. Dreis, D. Celebi, N. Schrickel, et al., Human serum albumin (HSA) nanoparticles: Reproducibility of preparation process and kinetics of enzymatic degradation, *Int. J. Pharm.* 347 (2008) 109–117, <https://doi.org/10.1016/j.ijpharm.2007.06.028>.
- [15] F. Kratz, Albumin as a drug carrier: design of prodrugs, drug conjugates and nanoparticles, *J. Contr. Release* 132 (2008) 171–183, <https://doi.org/10.1016/j.jconrel.2008.05.010>.
- [16] D.K. Eggers, Molecular confinement influences protein structure and enhances thermal protein stability, *Protein Sci.* 10 (2001) 250–261, <https://doi.org/10.1110/ps.36201>.
- [17] S. Curry, Lessons from the crystallographic analysis of small molecule binding to human serum albumin, *Drug Metabol. Pharmacokin.* 24 (2009) 342–357, <https://doi.org/10.2133/dmpk.24.342>.
- [18] D.C. Carter, J.X. Ho, Structure of serum albumin, *Adv. Protein Chem.* 45 (1994) 153–176, [https://doi.org/10.1016/S0065-3233\(08\)60640-3](https://doi.org/10.1016/S0065-3233(08)60640-3).

- [19] D. Caridha, D. Yourick, M. Cabezas, L. Wolf, T.H. Hudson, G.S. Dow, Mefloquine-induced disruption of calcium homeostasis in mammalian cells is similar to that induced by ionomycin, *Antimicrob. Agents Chemother.* 52 (2008) 684–693, <https://doi.org/10.1128/AAC.00874-07>.
- [20] T. Barupal, Y. Sompura, S. Sharma, Significant Role of Nanotechnology in Cancer and Molecular Genetics : an Overview, *Significant Role of Nanotechnology in Cancer and Molecular Genetics : an Overview*, 2022.
- [21] A. Sahu, W. Il Choi, G. Tae, Recent progress in the design of hypoxia-specific nano drug delivery systems for cancer therapy, *Adv. Ther.* 1 (2018), 1800026, <https://doi.org/10.1002/adtp.201800026>.
- [22] H. Dianat-Moghadam, M. HeydariFard, R. Jahanban-Esfahlan, Y. Panahi, H. Hamishehkar, F. Pouremamali, et al., Cancer stem cells-emanated therapy resistance: implications for liposomal drug delivery systems, *J. Contr. Release* 288 (2018) 62–83, <https://doi.org/10.1016/j.jconrel.2018.08.043>.
- [23] A. Dassonville-Klimpt, A. Jonet, M. Pillon, C. Mullié, P. Sonnet, Mefloquine derivatives: synthesis, mechanisms of action, antimicrobial activities, *Sci. against Microb. Pathog. Commun. Curr. Res. Technol. Adv. - I* 10275 (2011) 23–35.
- [24] K. Kaur, R. Kumar, S.K. Mehta, Nanoemulsion: a new medium to study the interactions and stability of curcumin with bovine serum albumin, *J. Mol. Liq.* 209 (2015) 62–70, <https://doi.org/10.1016/j.molliq.2015.05.018>.
- [25] G. Sekar, S. Wilson, A. Sivakumar, A. Mukherjee, N. Chandrasekaran, Elucidating the role of surfactant dispersed CNTs towards HSA fibrillation in vitro - a multiple spectroscopic approach, *J. Mol. Liq.* 221 (2016) 714–720, <https://doi.org/10.1016/j.molliq.2016.06.060>.
- [26] M. Sharma, B. Mann, R. Pothuraju, R. Sharma, R. Kumar, Physico-chemical characterization of ultrasound assisted clove oil-loaded nanoemulsion: as enhanced antimicrobial potential, *Biotechnol. Reports* 34 (2022), e00720, <https://doi.org/10.1016/j.btre.2022.e00720>.
- [27] W.J. Pichler, The important role of non-covalent drug-protein interactions in drug hypersensitivity reactions, *Allergy Eur. J. Allergy Clin. Immunol.* 77 (2022) 404–415, <https://doi.org/10.1111/all.14962>.
- [28] G. Sekar, S. Sugumar, A. Mukherjee, N. Chandrasekaran, Multiple spectroscopic studies of the structural conformational changes of human serum albumin — essential oil based nanoemulsions conjugates, *J. Lumin.* 161 (2015) 187–197, <https://doi.org/10.1016/j.jlumin.2014.12.058>.
- [29] Y. Liu, F. Ji, R. Liu, The interaction of bovine serum albumin with doxorubicin-loaded superparamagnetic iron oxide nanoparticles: Spectroscopic and molecular modelling identification, *Nanotoxicology* 7 (2013) 97–104, <https://doi.org/10.3109/17435390.2011.634079>.
- [30] G. Sekar, M. Haldar, D. Thirumal Kumar, C. George Priya Doss, A. Mukherjee, N. Chandrasekaran, Exploring the interaction between iron oxide nanoparticles (IONPs) and Human serum albumin (HSA): spectroscopic and docking studies, *J. Mol. Liq.* 241 (2017) 793–800, <https://doi.org/10.1016/j.molliq.2017.06.093>.
- [31] S.M. Huang, S.M. Liu, C.L. Ko, W.C. Chen, Advances of hydroxyapatite Hybrid organic composite used as drug or protein carriers for biomedical applications: a review, *Polymers* 14 (2022), <https://doi.org/10.3390/polym14050976>.
- [32] N. Nabila, N.K. Suada, D. Denis, B. Yohan, A.C. Adi, A.S. Veterini, et al., Antiviral Action of Curcumin Encapsulated in Nanoemulsion against Four Serotypes of Dengue Virus, 2020, pp. 54–62, <https://doi.org/10.2174/2211738507666191210163408>.
- [33] C. Vater, V. Hlawaty, P. Werdenits, M. Anna, V. Klang, A.E. Funding, et al., Effects of lecithin-based nanoemulsions on skin: short-time cytotoxicity MTT and BrdU studies, skin penetration of surfactants and additives and the delivery of curcumin, *Int. J. Pharm.* (2020), 119209, <https://doi.org/10.1016/j.ijpharm.2020.119209>.
- [34] M.C. Bonferoni, F. Riva, A. Invernizzi, E. Dellerà, G. Sandri, S. Rossi, et al., Alpha tocopherol loaded chitosan oleate nanoemulsions for wound healing. Evaluation on cell lines and ex vivo human biopsies, and stabilization in spray dried Trojan microparticles, *Eur. J. Pharm. Biopharm.* (2017), <https://doi.org/10.1016/j.ejpb.2017.11.008>.
- [35] G. Sekar, A. Sivakumar, A. Mukherjee, N. Chandrasekaran, Probing the interaction of neem oil based nanoemulsion with bovine and human serum albumins using multiple spectroscopic techniques, *J. Mol. Liq.* 212 (2015) 283–290, <https://doi.org/10.1016/j.molliq.2015.09.022>.
- [36] A. Journal, S. Issue, Formulation and Characterization of Plant Essential Oil Based Nanoemulsion : Evaluation of its Larvicidal Activity against *Aedes aegypti* ♀, vol. 25, 2013, pp. 18–20.
- [37] P. Mishra, J. Jerobin, J. Thomas, A. Mukherjee, N. Chandrasekaran, Study on antimicrobial potential of neem oil nanoemulsion against *Pseudomonas aeruginosa* infection in laboe rohita, *Biotechnol. Appl. Biochem.* 61 (2014) 611–619, <https://doi.org/10.1002/bab.1213>.
- [38] C.H. Anjali, Y. Sharma, A. Mukherjee, N. Chandrasekaran, Neem Oil (*Azadirachta indica*) Nanoemulsion - a Potent Larvicidal Agent against *Culex quinquefasciatus*, 2012, pp. 158–163, <https://doi.org/10.1002/ps.2233>.
- [39] S. Kentish, T.J. Wooster, M. Ashokkumar, S. Balachandran, R. Mawson, L. Simons, The Use of Ultrasonics for Nanoemulsion Preparation, vol. 9, 2008, pp. 170–175, <https://doi.org/10.1016/j.jifset.2007.07.005>.
- [40] M.H. Alkhatib, B.M. Binsiddiq, W.S. Backer, In vivo evaluation of the anticancer activity of a water-in-garlic oil nanoemulsion loaded with Docetaxel, *Int. J. Pharma Sci. Res.* 8 (2017) 5373–5379, [https://doi.org/10.13040/IJPSR.0975-8232.8\(12\), 5373-79](https://doi.org/10.13040/IJPSR.0975-8232.8(12), 5373-79).
- [41] S. Sugumar, J. Nirmala, H. Anjali, A. Mukherjee, N. Chandrasekaran, Bio-based Nanoemulsion Formulation , Characterization and Antibacterial Activity against Food-Borne Pathogens, 2012, pp. 1–10, <https://doi.org/10.1002/jobm.201200060>.
- [42] D.J. McClements, Y. Li, Structured emulsion-based delivery systems: Controlling the digestion and release of lipophilic food components, *Adv. Colloid Interface Sci.* 159 (2010) 213–228, <https://doi.org/10.1016/j.cis.2010.06.010>.
- [43] S. Zolghadri, A.A. Saboury, E. Amin, A.A. Moosavi-Movahedi, A spectroscopic study on the interaction between ferric oxide nanoparticles and human hemoglobin, *J. Iran. Chem. Soc.* 7 (2010) 145–153, <https://doi.org/10.1007/bf03246193>.
- [44] S.K. Burley, H.M. Berman, C. Christie, J.M. Duarte, Z. Feng, J. Westbrook, et al., RCSB Protein Data Bank: Sustaining a living digital data resource that enables breakthroughs in scientific research and biomedical education, *Protein Sci.* 27 (2018) 316–330, <https://doi.org/10.1002/pro.3331>.
- [45] F. Kiefer, K. Arnold, M. Künzli, L. Bordoli, T. Schwede, The SWISS-MODEL Repository and associated resources, *Nucleic Acids Res.* 37 (2009) 387–392, <https://doi.org/10.1093/nar/gkn750>.
- [46] S. Yuan, H.C.S. Chan, Z. Hu, Using PyMOL as a platform for computational drug design, *WIREs Comput. Mol. Sci.* 7 (2017), <https://doi.org/10.1002/wcms.1298>.
- [47] S. Kim, J. Chen, T. Cheng, A. Gindulyte, J. He, S. He, et al., PubChem 2019 update: improved access to chemical data, *Nucleic Acids Res.* 47 (2019) D1102–D1109, <https://doi.org/10.1093/nar/gky1033>.
- [48] J. Jerobin, R.S. Sureshkumar, C.H. Anjali, A. Mukherjee, N. Chandrasekaran, Biodegradable polymer based encapsulation of neem oil nanoemulsion for controlled release of Aza-A, *Carbohydr. Polym.* 90 (2012) 1750–1756, <https://doi.org/10.1016/j.carbpol.2012.07.064>.
- [49] V. Ghosh, A. Mukherjee, N. Chandrasekaran, Formulation and Characterization of Plant Essential Oil Based Nanoemulsion : Evaluation of its Larvicidal Activity against *Aedes aegypti* Formulation and Characterization of Plant Essential Oil Based Nanoemulsion : Evaluation of its Larvicidal Activity Aga, 2013.
- [50] A.A. Date, R. Dixit, M. Nagarsenker, Self-nanoemulsifying Drug Delivery Systems : Formulation Insights , Applications and Advances R Eview, vol. 5, 2010, pp. 1595–1616.
- [51] D. Press, Eucalyptus Oil Nanoemulsion-Impregnated Chitosan Film : Antibacterial Effects against a Clinical Pathogen , *Staphylococcus aureus*, 2015, pp. 67–75, in vitro.
- [52] H. Sis, M. Birinci, Effect of nonionic and ionic surfactants on zeta potential and dispersion properties of carbon black powders, *Colloids Surfaces A Physicochem. Eng. Asp.* 341 (2009) 60–67, <https://doi.org/10.1016/j.colsurfa.2009.03.039>.
- [53] S. Sugumar, V. Ghosh, M.J. Nirmala, A. Mukherjee, N. Chandrasekaran, Ultrasonics Sonochemistry Ultrasonic Emulsification of eucalyptus Oil Nanoemulsion : Antibacterial Activity against *Staphylococcus aureus* and Wound Healing Activity in Wistar Rats, vol. 21, 2014, pp. 1044–1049.
- [54] D. Pappas, B.W. Smith, J.D. Winefordner, Raman spectroscopy in bioanalysis, *Talanta* 51 (2000) 131–144, [https://doi.org/10.1016/S0039-9140\(99\)00254-4](https://doi.org/10.1016/S0039-9140(99)00254-4).
- [55] A. Flores, A. Malta, C. Pacheco, F. Baez, E. Ocampo, V. Conter, et al., Use of all-trans retinoic acid to treat acute promyelocytic leukemia: a case with very severe features at the onset in Nicaragua, 199604, *Med. Pediatr. Oncol.* 26 (1996) 258–260, [https://doi.org/10.1002/\(SICI\)1096-911X\(26:4<258::AID-MPO7>3.0.CO;2-I](https://doi.org/10.1002/(SICI)1096-911X(26:4<258::AID-MPO7>3.0.CO;2-I).